Electronic structure of semiconductor oxides: $InPO_4$, $In(PO_3)_3$, P_2O_5, SiO_2, $AlPO_4$, and $Al(PO_3)_3$

S. J. Sferco
Instituto de Desarrollo Tecnologico para la Industria Quimica, Guemes 3450, 3000 Santa Fe, Argentina

G. Allan, I. Lefebvre, and M. Lannoo
Laboratoire de Physique des Solides, Institut Supérieur d'Electronique du Nord, 41 Boulevard Vauban, 59046 Lille CEDEX, France

E. Bergignat and G. Hollinger
Laboratoire d'Electronique, Automatique et Mesures Electriques, Ecole Centrale de Lyon, Boîte Postale 163, 69131 Ecully CEDEX, France

(Received 30 March 1990)

The electronic structure of InP oxides, AlP oxides, and SiO_2 is investigated both experimentally and theoretically. X-ray-photoemission valence-band spectra are compared with tight-binding calculations in order to analyze the different contributions to each spectrum. Oxygen-oxygen interactions must be included to explain the experimental features. A systematic analysis of the SiO_2-$AlPO_4$-$InPO_4$ and $InPO_4$-$In(PO_3)_3$-P_2O_5 family evolution is made. The nature of the atomic states participating in the valence-band spectra is identified. The role of In and Al atoms in the valence band is analyzed, and we conclude that their influence is not negligible in the cases of $InPO_4$ and $AlPO_4$. We can distinguish two types of oxygen atoms in some oxides: O_b bridging different PO_4 tetrahedra, and O_{nb} only linked to one P atom. We conclude that the presence or absence of O_b has observable consequences in the XPS valence-band spectra.

I. INTRODUCTION

There is a general consensus today concerning the electronic-structure description of binary oxides such as SiO_2 and GeO_2.[1-4] The situation is quite different for the III-V semiconductor oxides, which are more complex. Several oxides can be grown for a given semiconductor. As an example, we consider InP, for which it is possible to get $InPO_4$ and $In(PO_3)_3$ oxides, but also P_2O_5 and In_2O_3. All these systems have different atomic structures and accordingly different electronic structures, as is reflected in their x-ray photoemission spectroscopy (XPS) valence-band spectra. For III-V semiconductor oxides, which have the α-quartz atomic structure, some general conclusions were given in Ref. 3. Extended Hückel band-structure calculations for some of the oxides we consider here have recently been given in Ref. 5, but no comparison with experimental XPS valence-band spectra was explicitly made.

Many aspects of interest have not been worked out to date. In particular, the differences in the XPS spectra when going from a group-IV oxide (such as SiO_2) to a III-V oxide (such as $AlPO_4$ or $InPO_4$) have not been explained and there is no evidence of any relation between the different local atomic environments and the XPS spectra. In this work we present a systematic study of different semiconductor oxides. Experimental XPS valence-band spectra for SiO_2, $AlPO_4$, $InPO_4$, $In(PO_3)_3$, $Al(PO_3)_3$, and P_2O_5 are first reported. Tight-binding (TB) band-structure calculations are also given in order to analyze the different contributions to the XPS spectra. A systematic comparison is made in order to understand the evolution in the total density of states going from SiO_2 to $AlPO_4$ and $InPO_4$, and from $InPO_4$ to $In(PO_3)_3$ and P_2O_5.

We focus our attention on the understanding of native InP oxides. They have a great importance in the passivation of InP semiconductors and they were exhaustively investigated[6-10] in order to use some of them for the fabrication of the metal-insulator-semiconductor field-effect transistor (MISFET). It was demonstrated that the nature of the oxides in InP, in particular the growth of $InPO_4$ or $In(PO_3)_3$, depends on the oxidation conditions.[6] It has been also shown that the $In(PO_3)_3$ oxide has better intrinsic passivating properties of InP surfaces than the other InP native oxides.[9] This oxide was recently used in the fabrication of MISFET devices.[11] In order to understand the nature of the electronic structure of oxides in general, we also include the analysis of SiO_2, $AlPO_4$, and $Al(PO_3)_3$ oxides as well.

We have used the TB approximations to perform band-structure calculations due to the large number of atoms in the unit cell, which goes from 9 atoms for SiO_2 to 78 atoms in $In(PO_3)_3$ and $Al(PO_3)_3$. This approach has the advantage of its simplicity both on the rapidity of calculation and on the interpretation of results. A similar approach was recently successfully applied to the study of the electronic structure and the Mössbauer isomer shift of antimony chalcogenides.[12-14]

The organization of this paper is as follows. Section II

describes some structural aspects of the oxides we have considered. Section III gives the experimental aspects concerning XPS valence-band spectrum measurements. Then Sec. IV is devoted to the theoretical approach. Section V develops the analysis of results, and conclusions are given in Sec. VI.

II. THE OXIDE ATOMIC STRUCTURE

In order to understand their electronic structure and the different features observed in the XPS valence-band spectra, we first recall the atomic structural arrangement of the different oxides under study.

We can consider all oxides as formed by structural units. These are (i) the SiO_4 tetrahedra for SiO_2, (ii) AlO_4 and PO_4 tetrahedra for $AlPO_4$, (iii) PO_4 tetrahedra and InO_6 (AlO_6) octahedra for $In(PO_3)_3$ [$Al(PO_3)_3$], and (iv) PO_4 tetrahedra for P_2O_5. Figure 1 shows a schematic representation of the different links between the structural units.

The structural arrangements of SiO_2 and $AlPO_4$ are identical. Each tetrahedron is linked to four other tetrahedra of the same type as in SiO_2 (Ref. 15) and of the other atom type in $AlPO_4$.[16] All links are made by oxygen atoms. The $InPO_4$ crystal consists of PO_4 tetrahedra and InO_6 octahedra packed together in such a way that there is no oxygen atom bridging two different tetrahedra.[17] The situation changes when going to $In(PO_3)_3$. This crystal consists of infinite chains of PO_4 tetrahedra with two oxygen atoms by tetrahedra linking different PO_4 tetrahedra. The other two oxygen atoms are linking InO_6 octahedra. Then we have two different P-O bonding distances for each tetrahedra as is indicated in Table I: the P-O_b (bridging: P-O_b-P) and P-O_{nb} (nonbridging P-O_{nb} $\cdots$ In).[18] The same situation holds for $Al(PO_3)_3$.[19] Finally, P_2O_5 consists of PO_4 tetrahedra linked together. In each PO_4 tetrahedron in P_2O_5, three oxygen atoms are shared with three neighboring tetrahedra. The last oxygen atom in the tetrahedron is linked to only one P atom.[20] Again there are two different P-O bonding distances. Table I summarizes all relevant distances for these oxides.

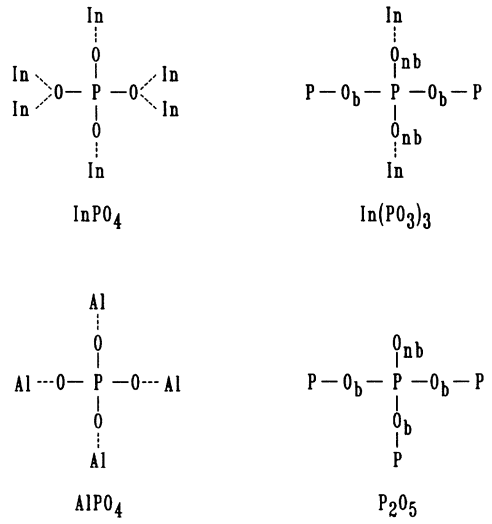

FIG. 1. Schematic atomic structure of semiconductor oxides. O_b and O_{nb}, respectively, are bridging and nonbridging oxygen atoms.

TABLE I. Mean atomic distances (in Å) for different semiconductor oxides.

SiO_2		$AlPO_4$		$InPO_4$[a]	
Si-O	1.61	P-O	1.52	P-O	1.56
		Al-O	1.73	In-O_1	1.97
				In-O_2	2.19
O-O	2.64	O-O	2.52	O-O	2.54
P_2O_5[b]		$Al(PO_3)_3$[b]		$In(PO_3)_3$[b]	
P-O_{nb}	1.49	P-O_{nb}	1.48	P-O_{nb}	1.47
P-O_b	1.56	P-O_b	1.57	P-O_b	1.58
		Al-O	1.88	In-O	2.12
O-O	2.52	O-O	2.49	O-O	2.49

[a]In $InPO_4$ there are two types of oxygen atoms. O_1 is associated to one P and one In atom, whereas O_2 is associated to one P and two In atoms.

[b]O_b stands for oxygen atoms bridging two PO_4 tetrahedra (P-O_b-P link). O_{nb} stands for nonbridging atoms as in P-O_{nb} $\cdots$ In for $In(PO_3)_3$, P-O_{nb} $\cdots$ Al for $Al(PO_3)_3$, and P-O_{nb} in P_2O_5.

III. EXPERIMENTAL DETERMINATION OF XPS VALENCE-BAND SPECTRA

The XPS spectra were recorded with a Hewlett-Packard 5950 Å spectrometer utilizing monochromatized Al $K\alpha$ rays (1486.6 eV). Under the conditions of the experiment, the Au $4f_{7/2}$ line measured at 84.0 eV had a full width at half maximum of 0.9 eV. Therefore, the instrumental response function is estimated to be equal to 0.6 or 0.7 eV.

Spectra for $InPO_4$, $In(PO_3)_3$, $Al(PO_3)_3$, and P_2O_5 were measured on powdered samples pressed on indium. The atomic structure of the three phosphate compounds was checked using x-ray diffraction. It is known that P_2O_5 reacts with air and the composition of our sample was estimated to be $P_2O_5-0.3\ H_2O$. $AlPO_4$ and SiO_2 were single crystals. They were cleaned by filing under nitrogen atmosphere. Using core-level spectroscopy, it was checked that the level of surface contaminants was low enough not to affect noticeably the valence-band structure.

Charging was detected on most of the samples and was compensated for by flooding low-energy electrons on the sample. As we were mostly interested in the shape of the valence-band spectra, we did not try to determine absolute binding energies referred to the Fermi level. The measured energies are referred to the top of the valence band.

IV. THEORETICAL MODEL

Our interest here is to perform band-structure calculations to obtain the partial and total density of states

(PDOS and DOS, respectively) for all oxides. The theoretical DOS may be compared directly with the XPS valence-band spectra concerning the energy positions of the peaks. The relative experimental intensity of the peaks depends on atomic cross sections and experimental resolution. The use of calculated atomic cross sections to compare the theoretical DOS with experiment will be discussed in Sec. V E. Then we focus our attention to the calculation of the DOS.

To perform band-structure calculations we use the empirical tight-binding method. This choice is principally due to the fact that we are studying oxides with a large number of atoms per unit cell. For example, $In(PO_3)_3$ and $Al(PO_3)_3$ oxides have 78 atoms in the unit cell. The tight-binding approach to the band-structure calculation is a well-documented procedure[21] that allows us to obtain much valuable information on the electronic structure of zinc-blende semiconductors[21] and that was recently extended to treat more complex systems, such as antimony chalcogenides.[12–14] We use a minimal basis set of atomic functions, consisting of one s and three p valence states for each atom. We also use (as is commonly done in TB calculations) the two-center approximation and assume that the atomic functions form an orthonormal basis set. In order to have a coherent description of all oxides, we use the same semiempirical law to parametrize the interatomic interactions. The simplest semiempirical expression for the hopping integrals is the well-known d^{-2} Harrison scaling law:

$$H_{i\alpha,j\beta}=\eta_{\alpha\beta}\frac{\hbar^2}{md^2}\ , \tag{1}$$

where d is the distance between atoms i and j. α and β stand for the atomic s or p orbitals of atoms i and j, respectively. The coefficients $\eta_{\alpha\beta}$ were empirically determined and their values are[22] $\eta_{ss}=-1.32$, $\eta_{sp}=1.42$, $\eta_{pp\sigma}=2.22$, and $\eta_{pp\pi}=-0.63$. The Harrison d^{-2} scaling law was proved to be correct for nearest-neighbor interactions in simple crystals, such as zinc-blende semiconductors, where all nearest-neighbor distances are the same. For the oxides in which we are interested, we have a distribution of close-neighbor distances and one knows from zinc-blende semiconductor band structures that the hopping integrals between next-nearest neighbors decrease faster than d^{-2}. So we take the same law that we have used to study complex systems such as antimony chalcogenides and has been proved to give for these materials very good agreement between the XPS spectra and the DOS.[13] For a given pair of atoms i and j, we define $\Sigma(i,j)$ as the sum of their atomic radii. The $\Sigma(i,j)$ values (also given in Table II) in fact are not very different from the nearest-neighbor distances (Table I). As for antimony chalcogenides, we use the following expression to calculate the interatomic interactions:

$$H_{i\alpha,j\beta}(d)=H_{i\alpha,j\beta}(\Sigma(i,j))\exp\left[-2.5\left[\frac{d}{\Sigma(i,j)^{-1}}\right]\right]\ , \tag{2}$$

where the preexponential factor looks like the Harrison d^{-2} law:

TABLE II. Atomic radii (in Å) taken from Ref. 23 and the $\Sigma(i,j)$ parameter equal to the sum of i and j atomic radii. The nearest-neighbor interatomic distances are given in Table I.

Element	Atomic radius	$\Sigma(i,j)$	
Al	1.18	Al-O	1.66
Si	1.11	Si-O	1.59
In	1.56	In-O	2.04
P	0.98	P-O	1.46
O	0.48	O-O	0.96

$$H_{i\alpha,j\beta}=\eta_{\alpha\beta}\frac{\hbar^2}{m(\Sigma(i,j))^2}\ . \tag{3}$$

A similar expression was successfully used to account for the electronic structure of a family of compounds, with a similar degree of complexity.[12–14] We use here the same cutoff distance $R_c(i,j)=1.4\Sigma(i,j)$ as used in Refs. 12–14 to take into account the extension of the atomic orbitals compared with the interatomic distance. For distances greater than R_c, the hopping interactions are neglected. The intra-atomic terms are taken from the Herman-Skillman atomic energies.[21]

When Eq. (2) is applied to calculate the band structure of the oxides, we cannot obtain a correct description of the XPS valence-band spectra (an example is given in Sec. V A, where we discuss the effect of the O-O interactions). Early works on SiO_2 (Refs. 4 and 24) demonstrate that it is necessary to introduce the nearest-neighbor O-O interactions in order to obtain a reasonable description of valence bands. Therefore, we have included O-O interactions between oxygen atoms belonging to the same PO_4 tetrahedron. The sum of atomic radii for two neutral oxygen atoms is 0.96 Å in Table II, and therefore the corresponding cutoff distance R_c should be equal to 1.34 Å. From Table I we see that considering these values, the O-O interactions should never be considered. However, due to electronic charge transfer to oxygen atoms in the oxide, and due to its greater electronegativity, we can expect a larger oxygen-atom radius. Then, we extend Eq. (2) for O-O interactions by fitting the atomic radius of oxygen in these oxides. We get a common value of 0.7 Å, larger than the neutral atomic radii 0.48 Å. Such a correction to the other atom radii has not been made as $\Sigma(i,j)$ remains close to the sum of the corresponding neutral atom radii.

The DOS obtained in this way, however, still presents two systematic discrepancies for all oxides: the gaps are strongly underestimated and the width of the valence band is systematically larger than the experimental one. This kind of result was also found in early works using the TB method for SiO_2.[4,24] It was found that it is necessary to shift upwards the Si orbital levels (relative to the oxygen orbital levels) by 4.5 or 7 eV, depending on the values used for the atomic levels. In our calculation the same situation holds not only for SiO_2, but also for all other oxides. It is necessary in particular to shift the P levels to get a good gap value for P_2O_5. A good agreement between DOS and XPS spectra as well as the gap values in all oxides can be obtained shifting upwards P

and Si levels by 6 eV relative to the oxygen levels. Orthogonalization of the Si and P states to the O states may account for such a shift. On the other hand, the In levels seem to remain constant relative to the oxygen levels. This could be explained by the fact that the In-O distances are larger than the P-O distances and so the orthogonalization between the In and O states leads to a much smaller shift.

To calculate the DOS, we have checked that eight special points[25] in the Brillouin zone for all systems except for $In(PO_3)_3$ and $Al(PO_3)_3$ are sufficient. For both oxides, due to the great number of atoms in the unit cell, one point is enough, and we take the Γ point. To compare with experimental spectra (Fig. 2), all levels have been broadened by a Gaussian of width equal to 0.5 eV. For the PDOS (Figs. 3–5), a 0.2 Gaussian width has been used to keep the PDOS structures.

Figure 2 shows, for all compounds, the DOS obtained from our band-structure calculations as well as the corresponding experimental XPS valence-band spectra. In order to understand the different contributions to the different peaks, we give in Figs. 3–5 the PDOS of $InPO_4$, $In(PO_3)_3$, and P_2O_5, respectively. They are representative

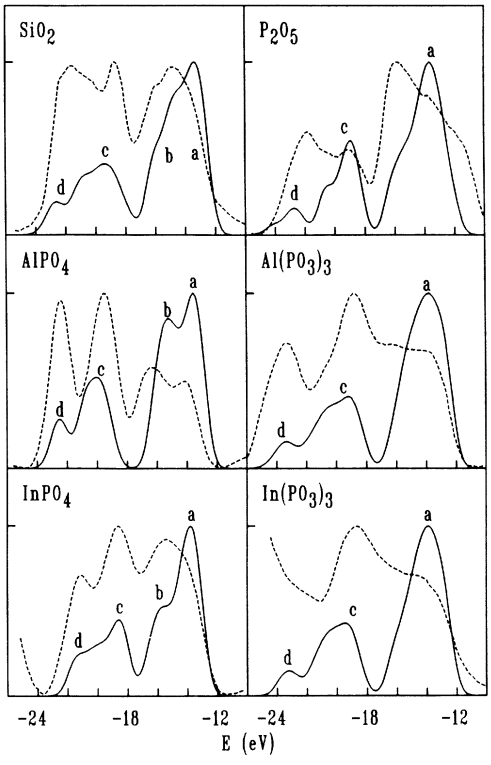

FIG. 2. Comparison of the experimental XPS spectra (dotted line) with the calculated densities of states (solid line). For each compound both curves are in arbitrary units and have been normalized to their maximum value. All DOS levels have been broadened by Gaussians of width equal to 0.5 eV. The experimental background has been subtracted except for $In(PO_3)_3$. In this case, the In 4*d* level overlaps the valence-band spectrum.

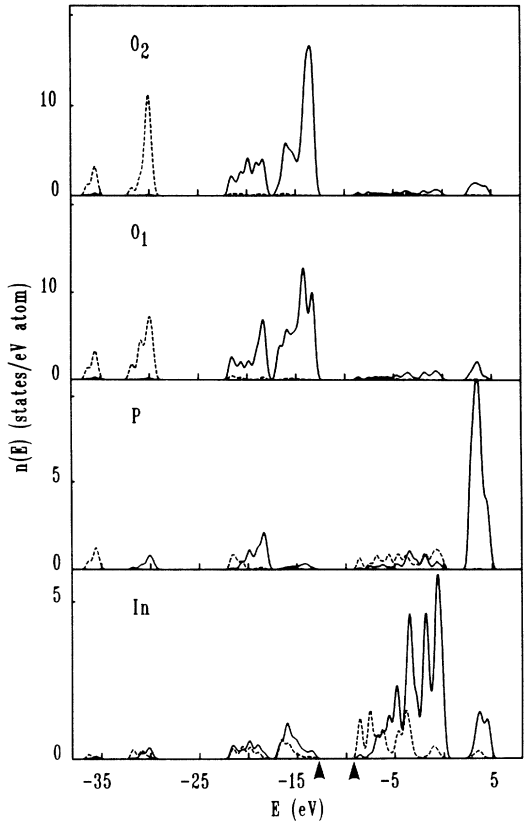

FIG. 3. Local $InPO_4$ densities of states. Each level has been broadened by a Gaussian of width equal to 0.2 eV: *s* states (dotted line) and *p* states (solid line). O_1 and O_2 are, respectively, the oxgyen atoms bonded to one and two In atoms (see Fig. 1). The arrows indicate the gap limits.

and the conclusions are also valid for the other oxides, as we discuss below.

V. DISCUSSION

We start our discussion by considering Fig. 2. For all the oxides we have studied, theoretical DOS curves show fairly good agreement with the XPS valence-band spectra. Several peaks are observed and can be assigned by looking at the PDOS. For $InPO_4$, $In(PO_3)_3$, and P_2O_5, they are shown in Figs. 3, 4, and 5, respectively.

The top of the valence band has a strong O 2*p* character for all oxides. This is consistent with earlier results obtained by TB works for SiO_2 (Refs. 1–4) and $AlPO_4$.[4] It corresponds to the peaks labeled *a* in Fig. 2 and arises at the O 2*p* atomic orbital energies. Then we can recognize in peaks *a* the well-known picture of "lone-pair" subbands for SiO_2 and $AlPO_4$.[1,4] Another peak (labeled *b*) is also obtained for SiO_2, $AlPO_4$, and $InPO_4$. It corresponds to the so-called "weak-bonding" subband.[1,4] For these three materials, the subbands *c* come from O 2*p* and P 3*p* orbital interactions (O 2*p* and Si 3*p* for SiO_2). Their lowest-energy subband *d* is made by O 2*p* and P 3*s* orbital interactions (O 2*p* and Si 3*s* for SiO_2).

For the other oxides $In(PO_3)_3$, $Al(PO_3)_3$, and P_2O_5, the

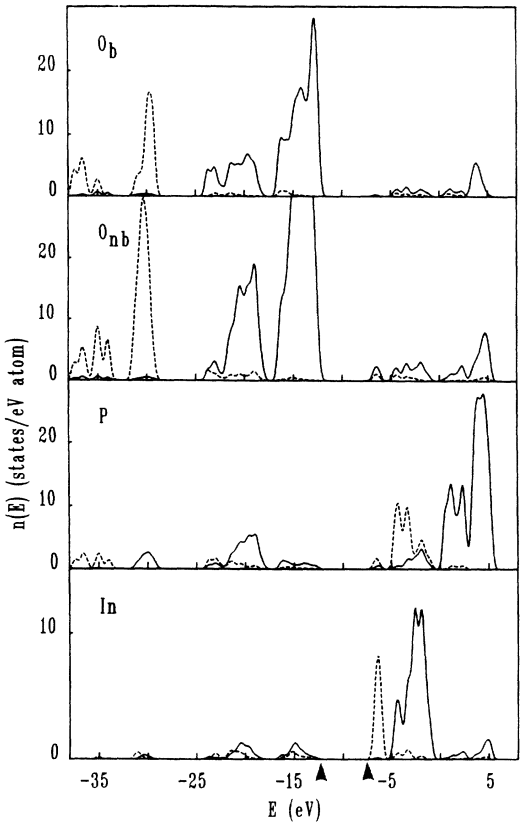

FIG. 4. Same as Fig. 3 for $In(PO_3)_3$. O_b and O_{nb} are, respectively, oxygen atoms bonding two PO_4 tetrahedra and nonbonding oxygen atoms (see Fig. 1).

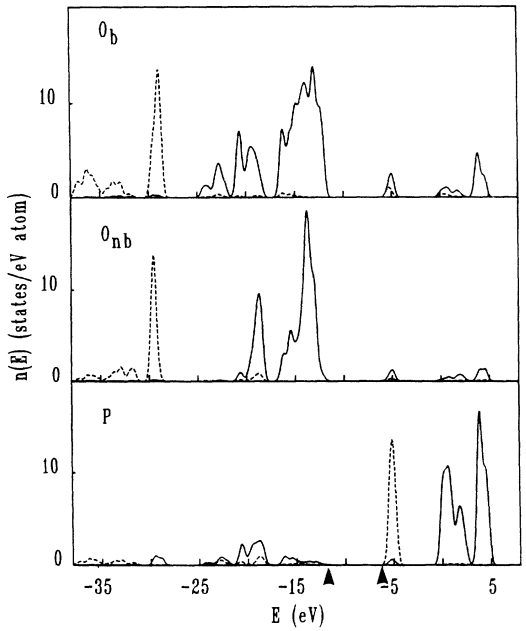

FIG. 5. Same as Fig. 3 for P_2O_5.

main contribution to subband *c* comes from O_{nb} 2*p* and P 3*p* orbital mixing. Their subbands *d* are then mostly due to O_b 2*p* and P 3*s* orbital interactions. It is interesting to discuss some features of the total DOS considering the structural arrangement of the atoms in the oxides.

A. SiO_2-$AlPO_4$-$InPO_4$ evolution

From a structural point of view, when we go from SiO_2 to $AlPO_4$, we replace two identical SiO_4 tetrahedra, linked by an oxygen atom, by two different tetrahedra: AlO_4 and PO_4 also linked by an oxygen atom. When we consider $InPO_4$ we must realize that the AlO_4 tetrahedra must be replaced by InO_6 octahedra conserving the PO_4 tetrahedra. These structural differences have consequences in the bonding distances as is shown in Table I. The Si-O distances in SiO_2 (1.61 Å) must be compared to the P-O (1.52 Å) and Al-O (1.73 Å) distances in $AlPO_4$, and with the P-O (1.56 Å) and In-O (1.97 Å) distances when we consider $InPO_4$. The P-O interactions are now the largest in these systems. This explains the nature of subbands *c* and *d* for the $AlPO_4$ and $InPO_4$ oxides compared to SiO_2: the "strong-bonding" band in SiO_2 (having *s* character at lower energies and *p* character at higher energies) is split into the two well-resolved peaks *c* and *d* for $AlPO_4$ and $InPO_4$. As stated before, peak *c* is basically resulting from O 2*p* and P 3*p* interactions, whereas peak *d* accounts for the O 2*p* and P 3*s* interactions. The Al or In state contributions to these subbands is negligible. More interesting is to understand why the $AlPO_4$ subbands *a* and *b* are experimentally resolved, whereas this is not the case in SiO_2 and $InPO_4$. From our results, two effects can be distinguished. The first one is the small but not negligible Al or In contribution to these subbands and the second one is the inclusion of the O-O interactions. From Table III we observe that the energy levels for Al and In are similar. Except for the change from AlO_4 tetrahedra to InO_6 octahedra, the only significant difference between $AlPO_4$ and $InPO_4$ is the variation of the Al-O distance (1.73 Å), which is smaller than the In-O distance (1.97 Å). Then hopping integrals between Al and O are larger than between In and O, shifting the level in $AlPO_4$ to lower energies. In fact, in the theoretical DOS of $AlPO_4$ and $InPO_4$, subbands *a* and *b* are distinguished, but not for SiO_2. Even if the Si-O distance is smaller than the In-O or Al-O distances, the reduction is compensated for by the energy difference between the Si and O levels, which is larger than the one between In or Al and O, leading to a small band near the

TABLE III. Atomic energies (in eV) used in this work. All energies are from Herman-Skillman values (Ref. 21). The P and Si levels have been shifted upwards by 6 eV in order to get better agreement with experimental XPS spectra and gap values.

	In	Al	P	Si	O
E_s	−10.12	−10.11	−11.10	−7.55	−29.14
E_p	−4.69	−4.86	−2.33	−0.52	−14.13

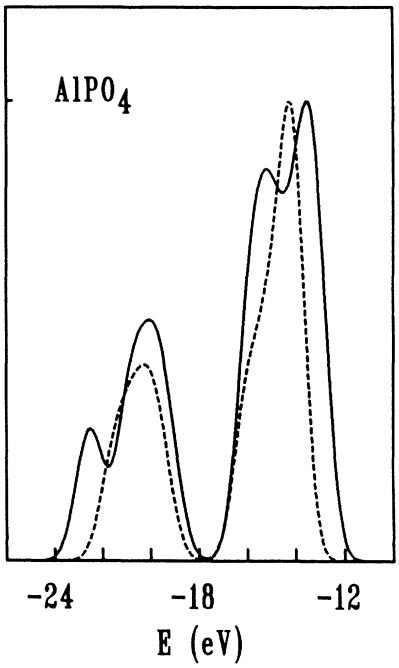

FIG. 6. Calculated valence-band densities of states with (solid line) and without (dotted line) O-O interactions. Both curves have been normalized to their maximum value.

lone pair peak.

Let us now consider the O-O interactions. Figure 6 shows their influence on the $AlPO_4$ valence-band structure. Its main effect is to broaden the peaks, in particular near the top of the valence band, and also to shift down in energy peaks *b* and *d*. In the DOS without O-O interactions, we can recognize in the shoulder on the left of the lone pair peak the presence of states due to Al-O interactions. But this splitting is more important when O-O interactions are properly included. Similar conclusions are valid for SiO_2 and $InPO_4$, although in these cases the effect seems less important than for $AlPO_4$. The O-O distance is almost the same in $AlPO_4$ and $InPO_4$ (2.52 and 2.54 Å, respectively). For SiO_2 this distance is equal to 2.64 Å and then the O-O interactions are slightly smaller. For SiO_2, this is not sufficient to split the subbands *a* and *b*, as it is in the case for $AlPO_4$. Finally, the absence of splitting between subbands *a* and *b* in the experimental spectrum for $InPO_4$ may be due to cross-section effects. This will be discussed in Sec. V E.

It is obvious from Fig. 6 that the inclusion of nearest-neighbor O-O interactions is necessary to account for the experimental features found in the valence-band XPS spectra.

B. $InPO_4$-$In(PO_3)_3$-P_2O_5 evolution

From $InPO_4$ to $In(PO_3)_3$, the atomic structure completely changes. The most important feature that appears is the presence of bridging oxygen atoms between different tetrahedra. Considering one tetrahedron, we have no bridging atom in $InPO_4$, two in $In(PO_3)_3$, and three in P_2O_5. The other oxygen atoms are linked to only one tetrahedron. In Fig. 2, we can observe that the width of the valence band is increased for systems having P-O_b-P links. This is due to a shift to lower energy of the peak *d* whose main contribution comes from O_b 2*p* and P 3*s* orbitals. The peak labeled *c* is also broadened. This is also due to the existence of P-O_b-P links in $In(PO_3)_3$ and P_2O_5. In the O_b PDOS (Fig. 5) this peak has two components. One arises at the same energy as the O_{nb} one. The other is obtained at lower energy due to a larger interaction between the O_b-P states and its two P neighbors.

Therefore the presence of P-O_b-P links is the natural explanation for the broadening of the experimental valence band when going from $InPO_4$ to P_2O_5. The width of the $In(PO_3)_3$ experimental spectrum will be discussed in the next section. O-O interactions also play a relevant role here. Their effect is more noticeable at the bottom than at the top of the valence band, where only a broadening of the peak occurs.

Some special considerations may be stated for P_2O_5. It crystallizes in three different forms. One of them is the *H* form, which is basically formed by packing together P_4O_{10} molecules.[26] The other two forms are orthorhombic varieties known as O forms and O′ forms[27] corresponding basically to the description we have made in Sec. II. The O form links ten PO_4 tetrahedra in a ring, whereas the O′ form links six PO_4 tetrahedra in a ring. The atomic positions were better determined for the O′ form and our calculations have been made for this variety of P_2O_5. On the other hand, the experimental spectrum was recorded on commercial P_2O_5 powder. This consists of a mixture of different forms including the amorphous one. Moreover, it is highly hygroscopic. This is the only oxide whose atomic structure was not verified prior to measuring the XPS spectrum. The atomic composition was estimated to be P_2O_5-0.3 H_2O. The presence of water, the possible presence of impurities, and the mixture of different varieties of P_2O_5 may be the origin of the differences found when comparing the experimental XPS spectra and the theoretical DOS, which has been calculated for the O′ form of P_2O_5. Differences concern principally the subband at the top of the valence band, which in the XPS spectrum is strongly wider than the theoretical DOS.

C. $In(PO_3)_3$ and $Al(PO_3)_3$ systems

These two oxides have a similar structural configuration giving crystals with exactly the same space group (*Ic*). The band-structure calculations give similar results but their experimental XPS spectra look very different (Fig. 2). This difference lies in the peak *d* near the bottom of the valence band. In fact, we obtain this peak at about the same energy for all systems having P-O_b-P links: P_2O_5, $In(PO_3)_3$, and $Al(PO_3)_3$). It is clearly observed for $Al(PO_3)_3$ but not for $In(PO_3)_3$. As discussed below, photoionization cross sections may have some importance, but a more plausible reason is the presence in $In(PO_3)_3$ of the very strong In 4*d* peak in the photoemission spectra below the bottom of the valence band. Due

to this peak, the subtraction of the background from the experimental spectrum is quite difficult. This In 4*d* peak is obviously not present in P_2O_5 and $Al(PO_3)_3$. This would explain why these oxides seem to have a wider valence band than $In(PO_3)_3$. On the other hand, the In 4*d* level that we have not considered in our calculation can also interact with the states at the bottom of the valence band, decreasing the width of the band. This effect would be less important for $InPO_4$ as the energy difference between the In 4*d* level and peak *d* is larger than the $In(PO_3)_3$ energy difference. We conclude that in $In(PO_3)_3$, the subband *d* at the bottom of the valence band exists, but is overlapped by the intense In 4*d* peak in the XPS spectra. Similar conclusions were found in Ref. 5.

D. The oxide conduction bands

First, we give in Table IV the calculated and experimental values for the gap of different oxides. One can see that with a 6-eV shift of the P levels the calculated values agree quite well with the experimental values. As stated before, the O 2*p* states form, in all oxides, the top of the valence band. For $InPO_4$ and $In(PO_3)_3$, the minimum of the conduction band has a strong In 5*s* character. Similar conclusions are valid for $AlPO_4$ and $Al(PO_3)_3$ concerning the Al 2*s* states. For SiO_2, the bottom of the conduction band has a strong Si 3*s* character. The top of the P_2O_5 gap is made of P 3*s* states. O-O interactions also play a role here, pushing down mainly the *s*-type levels in the conduction band (in a similar fashion as we found for the bottom of the valence band) and then lowering the gap value.

As is apparent from Figs. 3 and 4, the In states contribute mainly to the conduction band. Similar results are found for the Al states. Even if their participation in the valence band is not so important for O and P states, their influence is not negligible. Table V gives the calculated charges for all atoms in the oxides. For the In atom we obtain 1.59 e^- and 1.49 e^-, respectively, for $InPO_4$ and $In(PO_3)_3$. The Al states are occupied by 1.79 e^- in $AlPO_4$ and 1.36 e^- for $Al(PO_3)_3$. These values mean that the very simple description of In(Al) atoms as $In^{3+}(Al^{3+})$ cations is not correct.

TABLE IV. Calculated and experimental gap values (in eV).

	Calculated	Experimental
SiO_2	7.8	9[a]
$AlPO_4$	6.1	8[b]
$InPO_4$	3.8	4.5[c]–4.8[b]
$In(PO_3)_3$	5.6	5.5–6.8[d]
$Al(PO_3)_3$	5.5	
P_2O_5	6.6	8–10[c]

[a]Reference 28.
[b]Reference 29.
[c]Reference 30.
[d]References 9 and 31.

TABLE V. Calculated atomic charges (in electron units).

SiO_2		$AlPO_4$		$InPO_4$	
Si	1.46	Al	1.79	In	1.59
		P	1.86	P	1.85
O	7.27	O	7.08	O_1	7.07
				O_2	7.20
P_2O_5		$Al(PO_3)_3$		$In(PO_3)_3$	
		Al	1.36	In	1.49
P	1.78	P	1.90	P	1.91
O_b	7.18	O_b	7.18	O_b	7.17
O_{nb}	7.45	O_{nb}	7.23	O_{nb}	7.21

E. Cross sections

Reference 32 gives the calculated values of the free-atom photoionization cross sections corresponding to the excitation energy of XPS experiments. We may use these values to simulate the experimental spectra simply by multiplying the PDOS by the corresponding cross section and adding all of them to get the calculated spectra. Figure 7 shows the spectra calculated in this way for $InPO_4$, compared to the experimental spectrum and also compared to the calculated DOS. In Fig. 7, due to cross section, the P 3*s* states have been multiplied by 11.5 and the P 3*p* states by 2.5 by taking the O 2*p* states as reference.

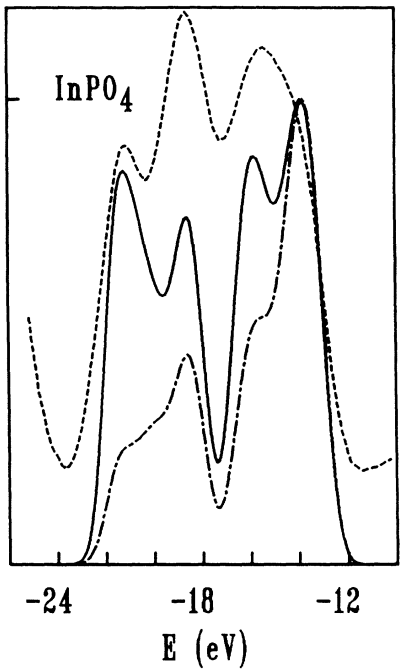

FIG. 7. Influence of photoionization cross sections on the calculated spectra. The dash-dotted line is the DOS without cross-section corrections and the solid line gives the result one gets when free atom cross sections (Ref. 32) are used. Both curves have been normalized to their maximum value. For comparison, the experimental result is given by the dotted line and has been shifted upwards.

Comparison between the theoretical DOS and the XPS spectra reveals that *s*-type states must effectively be raised relative to oxygen *p* states. Figure 7 shows fairly good agreement for the peak at the bottom of the valence band, but the agreement is not as good for the peak near the middle of the valence band. This is probably due to the fact that atoms in solid do not necessarily have the same cross sections as free atoms. This result seems to be valid for all oxides. So we conclude that such atomic cross sections must be used with caution. They must be taken only as a guide in order to have some insight concerning the possible experimental spectra.

VI. CONCLUSION

We have presented a comparison between the experimental XPS spectra and the theoretical DOS valence band for several semiconductor oxides. In order to have a coherent description of all oxides, we have developed an empirical TB model that allows us to understand many features of the experimental XPS spectra. We are able to identify the states contributing to different experimental peaks and correlate the structural differences between oxides with the nature of the states present in each valence subband. We can summarize our results as follows.

(i) It is necessary to include the O-O interactions in order to have a correct description of XPS spectra.

(ii) All oxides have O $2p$ states forming the top of the valence band.

(iii) The lowest-energy peak at the bottom of the valence band corresponds to interactions between O $2p$ and P $3s$ state interactions.

(iv) The peak at the middle of the band is due to interactions between O $2p$ and P $3p$ states.

(v) The experimental splitting of the peak near the top of the valence band in $AlPO_4$ is due to the presence of Al-O and O-O interactions.

(vi) In $In(PO_3)_3$ the peak at the bottom of the valence band (fingerprint of $P\text{-}O_b\text{-}P$ links) is overlapped in the XPS spectra by the intense In $4d$ peak.

(vii) Systems having links $P\text{-}O_b\text{-}P$ have a greater valence-band width than systems where these links do not exist.

ACKNOWLEDGMENTS

We thank J. Durand for providing the samples. This work was supported by the Cooperation Program between Consejo Nacional de Investigaciones Científicas y Técnicas (CONICET) (Argentina) and Centre National de la Recherche Scientifique (CNRS) (France). The Laboratoire de Physique des Solides and the Laboratoire d'Electronique, Automatique et Mesures Electriques are "Unité Associée au centre National de la Recherche Scientifique Nos. 253 and 848."

[1]S. T. Pantelides and W. A. Harrison, Phys. Rev. B **13**, 2667 (1976).

[2]J. R. Chelikowsky and M. Schluter, Phys. Rev. B **15**, 4020 (1977).

[3]M. Bensoussan and M. Lannoo, J. Phys. (Paris) **40**, 49 (1979).

[4]R. B. Laughlin, J. D. Joannopoulos, and D. J. Chadi, Phys. Rev. B **20**, 5228 (1979).

[5]A. Le Beuze, R. Lissilour, A. Quemerais, D. Agliz, R. Marchand, and H. Chermette, Phys. Rev. B **39**, 11 055 (1989).

[6]G. Hollinger, E. Bergignat, J. Joseph, and Y. Robach, J. Vac. Sci. Techol. A **3**, 2082 (1985).

[7]G. Hollinger, G. Hughes, F. J. Himpsel, J. L. Jordan, J. F. Morar, and F. Houzay, Surf. Sci. **168**, 617 (1986).

[8]E. Bergignat, G. Hollinger, and Y. Robach, Surf. Sci. **189/190**, 353 (1987).

[9]G. Hollinger, J. Joseph, Y. Robach, E. Bergignat, B. Commere, P. Viktorovitch, and M. Froment, J. Vac. Sci. Technol. B **5**, 1108 (1987).

[10]G. Hollinger, C. Estrada, J. Durand, and M. Gendry, J. Microsc. Spectros. Electron. **13**, 31 (1988).

[11]A. Falcou, G. Post, P. Viktorovitch, R. Blanchet, K. Choujaa, G. Hollinger, Y. Robach, and J. Joseph, in *Proceedings of the Conference on Indium Phosphide and Related Materials for Advanced Electronic and Optical Devices,* edited by R. Singh and L. J. Mersick (SPIE, Washington, D.C., 1989).

[12]I. Lefebvre, M. Lannoo, G. Allan, A. Ibanez, J. Fourcade, J. C. Jumas, and E. Beaurepaire, Phys. Rev. Lett. **59**, 2471 (1987).

[13]I. Lefebvre, M. Lannoo, G. Allen, and L. Martinage, Phys. Rev. B **38**, 8593 (1988).

[14]J. Olivier-Fourcade, A. Ibanez, J. C. Jumas, M. Maurin, I. Lefebvre, P. Lippens, M. Lannoo, and G. Allan, J. Solid State Chem. **87** 366 (1990).

[15]R. W. G. Wyckoff, in *Crystal Structures* (Wiley, New York, 1965), Vol. 1.

[16]M. Goiffon, G. Bayle, R. Astier, J. C. Jumas, E. Philippot, and M. Maurin, Rev. Chim. Miner. **20**, 338 (1983).

[17]R. C. L. Mooney, Acta Crystallogr. **9**, 113 (1956).

[18]J. Bentama, J. Durand, and L. Cot, Z. Anorg. Allg. Chem. **556**, 227 (1988).

[19]H. van der Meer, Acta Crystallogr. B **32**, 2423 (1976).

[20]D. W. J. Cruickshank, Acta Crystallogr. **17**, 679 (1964).

[21]W. A. Harrison, in *Electronic Structure and Properties of Solids* (Freeman, San Francisco, 1980).

[22]W. A. Harrison, Phys. Rev. B **24**, 5835 (1981).

[23]E. Clementi, D. L. Raimondi, and W. P. Reinhardt, J. Chem. Phys. **47**, 1300 (1967).

[24]E. P. O'Reilly and J. Robertson, Phys. Rev. B **27**, 3780 (1983).

[25]D. J. Chadi and M. L. Cohen, Phys. Rev. B **8**, 5747 (1973).

[26]D. W. J. Cruickshank, Acta Crystallogr. **17**, 677 (1964).

[27]J. R. Van Wazer, in *Phosphorus and its Compounds* (Interscience, New York, 1958), Vol. 1.

[28]T. H. DeStefano and D. E. Eastman, Phys. Rev. Lett. **27**, 1560 (1971).

[29]A. Elhaidouri, Ph.D. thesis, Université des Sciences et Techniques du Languedoc, Montpellier, France, 1987 (unpublished).

[30]*Physics and Chemistry of III-V Compound Semiconductor Interfaces,* edited by C. W. Wilmsen (Plenum, New York, 1985), p. 182.

[31]G. Leveque, unpublished results.

[32]J. H. Scofield, J. Electron. Spectrosc. **8**, 129 (1976).